BIOMATERIALS FOR THE CENTRAL NERVOUS SYSTEM

Contract No. NO1-NS-1-2338

Quarterly Progress Report #6

April 30, 2003

The University of Michigan and
The University of Utah

David C. Martin and Patrick A. Tresco

Quarterly Progress to:	National Institute of Health
Contract Monitor:	William Heetderks, Ph.D.
Research Contract	"Biomaterials for the Central Nervous System"
Contract No.	NO1-NS-1-2338
Principal Investigators:	David C. Martin and Patrick A. Tresco
Date:	April 30, 2003

Overview

This report is a summary of our activity in the sixth quarter of our contract, corresponding to the period from January 31, 2003 to April 30, 2003. We discuss our work to develop polymer films for the surface modification of neural prosthetic devices and the *in vitro* and *in-vivo* testing of these modified electrodes.

In this quarterly report we discuss results on the coating of polypyrrole-nerve growth factor composites on the surface of neural probes. We also discuss the deposition of synthetic hydrogels of poly(vinyl alcohol), and confirm the ability to polymerize polypyrrole in these synthetic hydrogel scaffolds. Finally, we show that the conducting polymers PEDOT and PPy can be grown into morphologies consisting of microtubules and microspheres. Since these structures may be able to encapsulate and subsequently release biologically functional molecules in a well-controlled fashion, they are of considerable interest for this application. We also include a compilation of the measurements of impedance as a function of deposition charge (thickness) for a variety of polymer films deposited on neural electrodes in our laboratory.

The Tresco group reports quantitative measurements of the biological response of coated, hydrogel coated, and lyophilized hydrogel coated probes. These results indicated that there is no significant difference in GFAP immunoreactivity between various hydrogel coated probes compared to control. However, there is a significant reduction in neurofilament immunoreactivity for distances up to 200 microns around implanted tethered electrodes.

Synthesis and Characterization of Polypyrrole-Nerve Growth Factor Composites for Neural Probes

1. Introduction

Over the years, microelectrodes have proved to be inadequate for long-term implantation, and many works have been done with preventing the cellular encapsulation playing a significant role in limiting neural communication. Conducting electro-active polymers including polypyrrole, polyaniline, and polythiophene have been used to modify biosensors and bioelectronics [1, 2]. Out of these conducting polymers, polypyrrole has been widely studied due to its aqueous solubility and low oxidation potentials of the monomer, high conductivity, and compatibility with mammalian cells [3]. Polystyrene sulfonate was chosen as the dopant materials because of its stability and biocompatibility. Neurotrophins are critical for the development and maintenance of the peripheral and central nervous system [4]. These growth factors control cell survival, differentiation, growth cessation, and apoptosis. The biologic function makes them of therapeutic interest for the treatment of a number of neurodegenerative diseases. Nerve Growth Factor (NGF), one of the neurotrophins, such as Brain-Derived Neurotrophic Factor (BDNF), Neurotrophin-3 (NT-3), Neurotrophin-4/5 (NT-4/5) and Neurotrophin-6, is the best characterized and widely used. It is well known that it promotes the survival and differentiation of sensory and sympathetic neurons [5]. By incorporating of NGF in the Polypyrrole conducting polymer, the performance of these devices could, presumably, be improved by promoting better integration within the nervous system and minimizing the host response.

Experimental

2-1. Materials

The pyrrole monomer and poly(sodium-4-styrene sulfonate) (PSS) were purchased from Aldrich and used without any prior purification. Nerve Growth Factor (NGF 7S, murine, natural, cat# 13290-010) was from Invitrogen (Carlsbad, CA). All other chemicals were purchased form Sigma (St. Louis, MO) unless otherwise stated.

2-2. Material preparation

The composite of Polypyrrole, PSS, and NGF was grown galvanostatically on the gold or iridium electrode sites (1250 μm^2 in area) of a neural probe. The electrical supply was an Autolab PGSTAT12. This is a potentiostat / galvanostat with a compliance voltage of 12 V, especially dedicated for research in solutions with low resistance, i.e. aqueous solutions. Maximum current is limited to 250 mA and current resolution is 30 fA on the 10 nA current range. It also offers the possibility to do iR compensation (both i-Interrupt and Positive Feedback). The reaction was performed in a two-electrode cell. The impedance was measured in the three-electrode cell setup. A platinum foil was used as the counter electrode and a saturated calomel electrode (SCE) was used as the reference electrode. A site on the probe was used as the working electrode. The monomer solution (1 ml) contains 12.7 µl pyrrole monomer, 200 mg PSS and NGF (50 µg/ml). The solution was purged with N_2 for approximately 10 minutes to prevent the oxidation of monomer before use. In the galvanostatic mode, a current density of 8 mA/cm^2 was used. The amount of material deposited onto the electrode site was controlled by deposition time and current applied.

2-3. Impedance spectroscopy measurements

An FRA2 electrochemical impedance system was used to obtain impedance spectra of the electrode sites. It is used for Electrochemical Impedance Spectroscopy (EIS) in the frequency range from 10 µHz to 1 MHz. Impedance measurements can be performed by applying a pure sine wave or using the multi-sine signal consisting of five or fifteen frequencies. The measurements can be done at a single potential, which can be the open circuit potential, but a frequency scan may also be repeated at every potential during a potential or current scan, or by measuring the impedance as a function of time. A potential scan measurement can for example be used for the determination of the double layer capacitance versus potential or to make a Mott Schottky plot. A solution of 0.1 M phosphate buffer solution (pH = 7) was used as the electrolyte in a three-electrode cell. An AC sinusoidal signal of 5 mV amplitude was used and the DC potential was set to 0 V. The value of the impedance was determined at the range of 10-100,000 Hz.

2-4. Cyclic voltammetry

Cyclic voltammetry (CV) was performed using a PGSTAT12 potentiostat / galvanostat. The three-electrode cell setup was the same as that used for impedance spectroscopy. A scan rate of 100 mV/s was used and the potential on the working electrode was swept between –0.9 to 0.5 V vs. SCE. These limits were wide enough to

include the reversible redox reaction and narrow enough to avoid over-oxidation and remain within the water window. Before each CV was recorded, two cycles were swept to ensure that the film reached its stable state.

2-4. FT-IR (Fourier Transform Infra-Red spectroscope)

By using a Perkin-Elmer Spectrum GX attached with a Perkin-Elmer Multi-microscope, FT-IR spectroscopy was performed in order to characterize the chemical composition of the polypyrrole / nerve growth factor composite. This machine is equipped with a liquid nitrogen cooled MCT detector. This microscope accessory enabled focusing on a small area of the sample such as a neuronal probe. The scanning area was set as 36× 36 μm^2. A probe sample was placed on a gold mirror, and the background reflection signal from gold mirror was collected and calculated before scanning samples. The samples were scanned 100 times in the range of 4000 to 750 cm^{-1}. Perkin-Elmer's Spectrum Software Version 3.01 was used to generate the FTIR spectrum.

3. Results and discussion

We have successfully produced composite films with pyrrole, polystyrene sulfonate and nerve growth factor to enhance the electrical and biological properties of the electrode sites on the neural probe. Although nerve growth factor could be itself used as the counter ion, to increase the efficiency of electro-chemical polymerization process PSS was also used as co-counter ion. Fig. 1 shows low magnification SEM images of the coating after various deposition times.

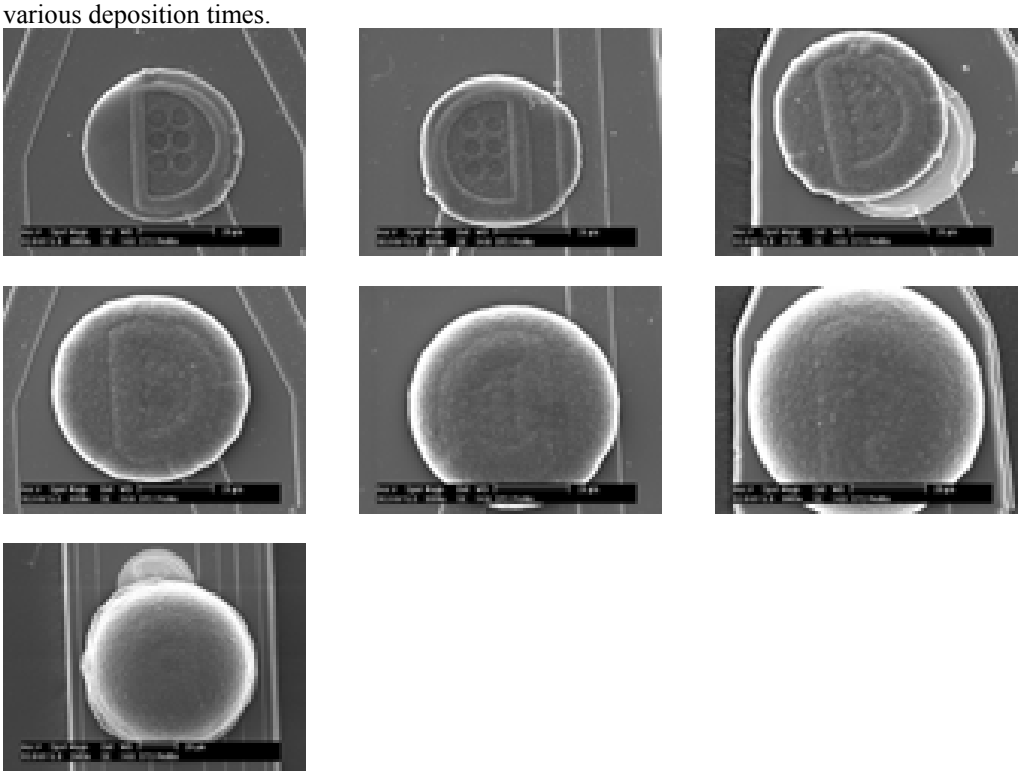

Fig. 1 (a) 3 μC (30 sec@100nA), (b) 6 μC (1 min@100 nA), (c) 18 μC (3 min@100 nA), (d) 42 μC (7 min@100 nA), (e) 60 μC (10min@100 nA), (f) 120 μC (20 min@100 nA), (g) 360 μC (60 min@100 nA).

Fig. 2 shows the microstructure of these coatings at higher magnification. The surface structure seen in the SEM did not change dramatically, but there was a consistent increase in the thickness of the over all film increase with the amount of applied charge. The impedance of these films, however, decreases dramatically with charge during the intial stages of deposition, and then increases when the film is sufficiently thick (Fig. 3). This phenomena has now been observed in a number of different coatings prepared in our laboratory, as summarized in the enclosed plot. We are currently working on models to explain this behavior. In the past we have rationalized this as due to an increase in the effective surface area of the coating with thickness leading to a decrease in impedance, followed by an increase in impedance as the films get thicker.

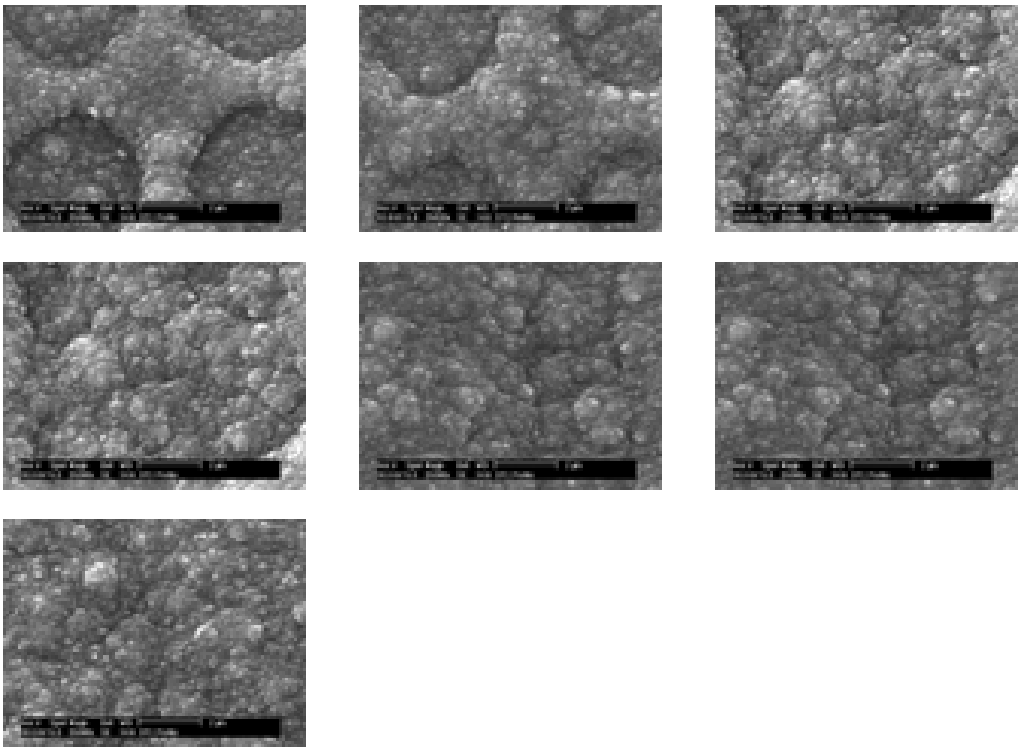

Fig. 2. a) 3 μC (30 sec@100nA), (b) 6 μC (1 min@100 nA), (c) 18 μC (3 min@100 nA), (d) 42 μC (7 min@100 nA), (e) 60 μC (10min@100 nA), (f) 120 μC (20 min@100 nA), (g) 360 μC (60 min@100 nA).

Figure 4 shows the variation of impedance magnitude at 1 kHz as a function of deposition time, showing similar behavior of the impedance properties with PPy-PSS composite. This is not surprising, since the amount of nerve growth factor is fairly small compared with the amount of PSS in the raw monomer source solution. It could be assumed that the property of polypyrrole / PSS is dominant in this composite and NGF does not significantly affect the electrical property of this composite. A certain intermediate amount of charge (20-60 μC) on the electrode gave the lowest impedance at 1 kHz. Figure 5 shows a plot of impedance as a function of charge at different currents, indicating that the rate of deposition did not have a pronounced effect on behavior under these conditions.

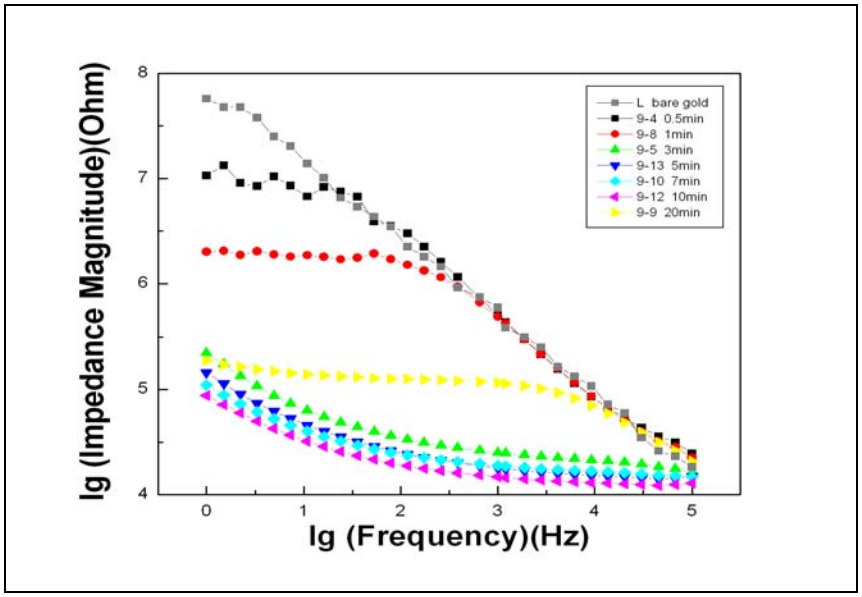

Fig 3. Impedance Spectroscopy of the Composite of PPy-PSS-NGF with spectrum of frequency.

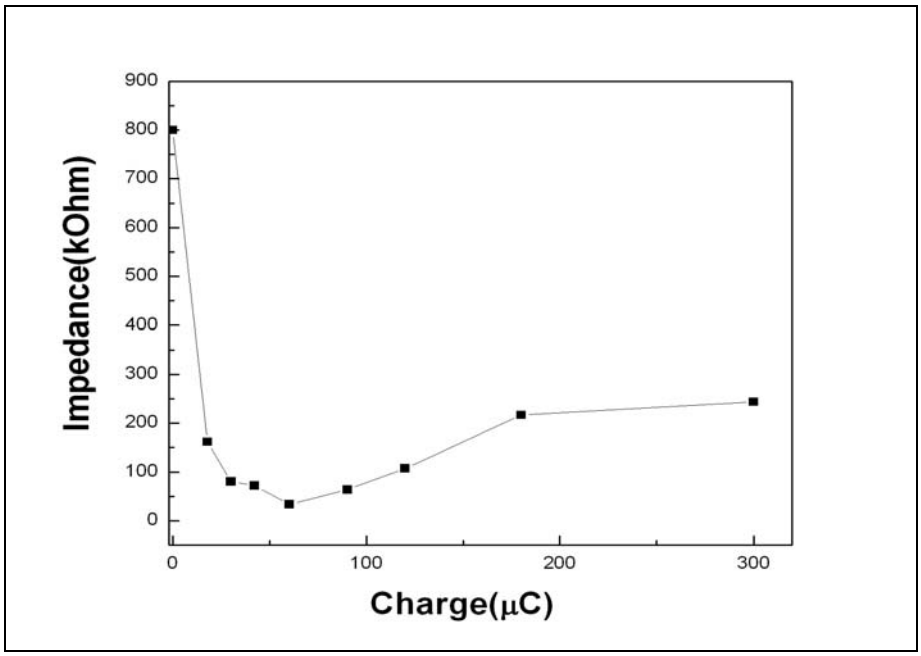

Fig. 4. Impedance of the Composite of PPy-PSS-NGF at 1 kHz as a function of deposition time.

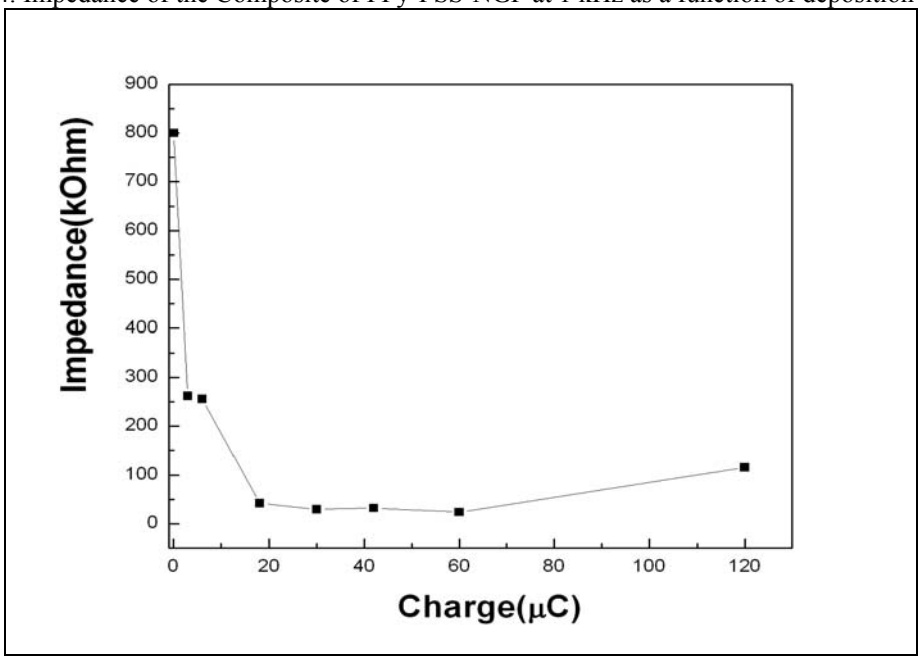

Fig. 5. Impedance of the Composite of PPy-PSS-NGF at 1 kHz as a function of deposition current.

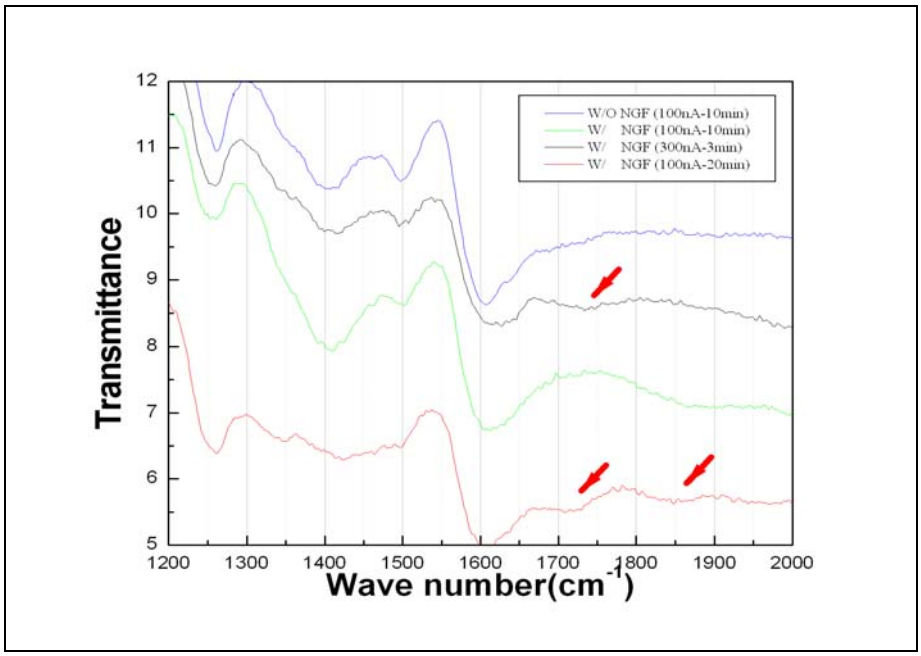

Fig. 6 FTIR of PPy/PSS/NGF coated neural probe. The indicated peaks correspond to the Amide I and II absorptions from the NGF polypeptide.

FT-IR spectroscopy was performed in order to characterize the chemical composition of the polypyrrole / nerve growth factor composite. This microscope is equipped with liquid nitrogen cooled MCT detector enabled focusing on a small area of the sample such as a neuronal probe. Figure 6 shows the IR spectrum of polypyrrole / nerve growth factor composite compared with polypyrrole coating without nerve growth factor. The blue line corresponds to the polypyrrole / PSS coating without nerve growth factor. A black line shows the IR spectrum of polypyrrole / nerve growth factor composite. Finally, a green and red line indicates that IR spectrum of polypyrrole / nerve growth factor composite with applying excess current to these samples. Polypyrrole doped with PSS and nerve growth factor (black line) had an absorption band at 1750 cm^{-1}, which comes from Amide I and II while polypyrrole doped with only PSS (blue line) does not. The red and green lines show peaks whose positions are somewhat different from the polypyrrole doped with PSS and nerve growth factor, suggesting that protein in these samples is deformed to some extent during deposition. Nevertheless this clearly shows the existence of protein in these composites.

References

1. Bimolecular immobilization on electrode surfaces by entrapment of attachment to electrochemically polymerized films A review Biosen. Bioelectron. 14 1999 443-456
2. Chemical and biological sensors based on electrically conducting polymers hand book of conducting plymers A Guiseppi-Elie, G.G Wallace T. Matsue 1998.
3. Stimulation of neurite outgrowth using an electrically conducting polymer, C.E. Schmidt, V.R. Shastri, J.P. Vacanti, R. Ranger, Proc. Natl. Acad. Sci. U.S.A 94 1997 8948-8953.
4. Nerve growth factor: structure and function, Wiesmann C, de Vos AM, Cellular and molecular life sciences, 58 (5-6): 748-759 MAY 2001
5. Nerve growth factor signaling, neuroprotection, and neural repair, Sofroniew MV, Howe CL, Mobley WC, Annual review of neuroscience, 24: 1217-1281 2001

Electrochemical Deposition of Conducting Polymers within Synthetic Hydrogels on Microelectrode Sites

Abstract

The use of polypyrrole (PPy) as a conducting polymer has been under investigation for many years. While the polymer itself has poor conductivity. pyrrole monomer must be doped and electrochemically polymerized by counter ion such as, poly(styrene sulfonate) (PSS), CLO_4^-, or biological molecules such as NGF. Counter ion can be bonded by electro-static forces to the backbone of polymer chains. PSS molecule is larger than CLO_4^- and the hypothesis is that PPy / CLO_4^- is more conductive than Ppy/PSS. It has been shown by using synthetic or natural hydrogel polymers conductivity will increase that it has depended on nature of hydrogel and water content percentage.

Alginate (natural hydrogel) chains can be cross-linked by Ca ions. Because of cross-link nature, in aqueous solution with lower concentration of Ca ions, Ca ions migrate in direction of gradient and alginate chain will be released from surface of neural probes. On the other hand, synthetic hydrogels such as poly(acrylic Acid) (PAAc), Poly (vinyl alcohol) PVA, Poly (hydroxy ethyl methacrylate) (PHEMA) can be cross-linked covalently. Better mechanical properties and keeping hydrogel structure in different ions solutions are expected from these materials. Also synthetic hydrogels can shrink or expand when exposed to external electrical stimulation. Therefore, this property makes them of interest for drug delivery systems.

Poly(vinyl alcohol) is biocompatible polymer that can be cross-linked covalently by chemical agents such as N, N' methylene bisAcrylamide (MBA) and sodium tetraborate (Borax). The cross-linking mechanism is the following:

- Borax hydrolyzes in water to produce boric acid and the OH-ion

  $B_4O_7^{-2}(aq) + 7\ H_2O$ — $4\ H_3BO_3\ (aq) + 2\ OH^-(aq)$

- The boric acid further reacts with water to form a borate anion.

  $H_3BO_3\ (aq) + 2\ H_2O$ — $B(OH)^{4-}(aq) + H_3O+(aq)$

- The tetrahedral borate ion crosslinks with the poly(vinyl alcohol)

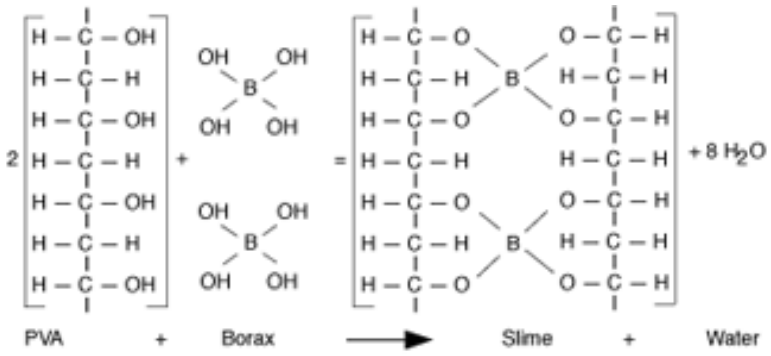

Materials and methods

Electrochemical deposition of PPy/PSS through PVA hydrogel

Pyrrole monomer 98%, PSS, PVA (Mw 124,000-186,000) and sodium tetraborate were purchased from Sigma. A solution of 0.2 M pyrrole has been prepared by dissolving 73.9 µl of pyrrole monomer in 5 ml of de-ionized water under stirring condition. Also 0.1 M PSS solution has been prepared. Poly(vinyl alcohol) 4% solution was prepared by dissolving 0.4 gm PVA in 10 ml DI water under stirring and 80 C conditions. Also 0.4 gm of Borax was dissolved in 10 ml DI water to make a 4% solution.

The PVA solution was gelled and cross-linked around of shank of probes by dipping method. The thickness of hydrogel coated could be controlled by number of dips inside the hydrogel solution. Pyrrole monomer has been polymerized and deposited on the gold sites of neural probes by Gamry Instrument in Galvanostat mode at 5 nA and 10 nA. The hydrogel /Ppy /PSS composite morphology was observed by using optical microscopy and conductivity has been measured by impedance spectroscopy.

Results

The thickness of hydrogel around the probe shank varied depending on the PVA and Borax concentrations, and the number and times of dipping into the PVA solution. In these particular experiments, in the hydrated state the nominal thickness was 42 μm and in dehydrated state was 19 μm. Polypyrrole was polymerized inside the hydrogel scaffolds as shown in the optical micrographs.

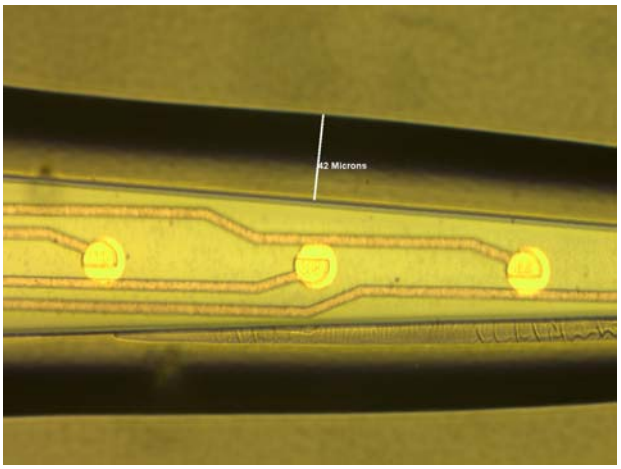

Fig. 7: Hydrated hydrogel, Thickness = 42 μm

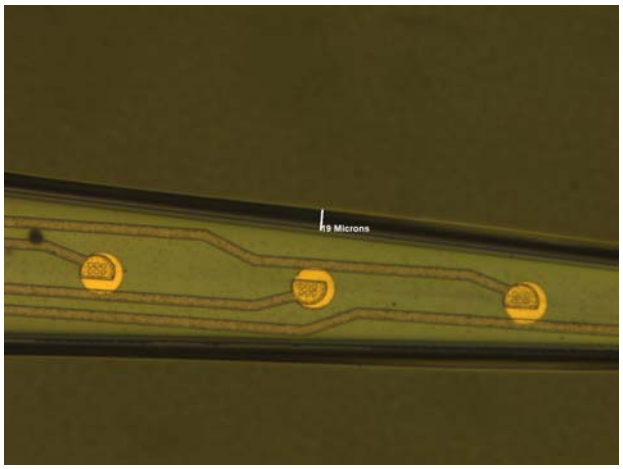

Fig 8: Dehydrated hydrogel, Thickness = 19 μm

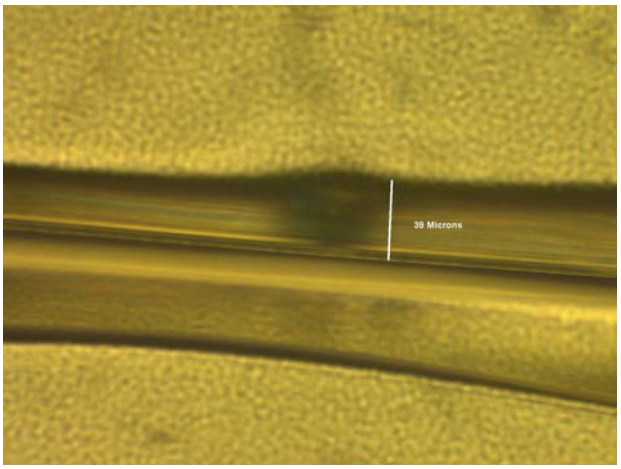

Fig. 9: I = 5 nA and t =60 min

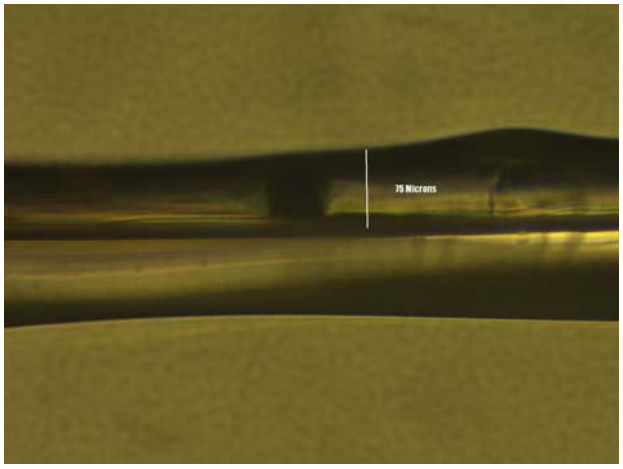

Fig. 10: I = 10 nA and t =60 min

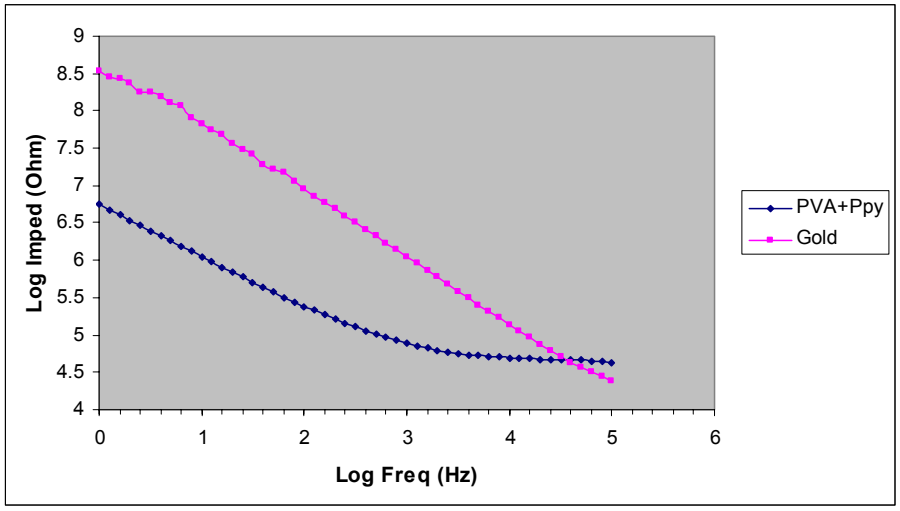

Fig. 11: Impedance at 1 kHz: for Gold 1.4 MΩ and for PVA/Ppy/PSS 77 kΩ

Surfactant-mediated Fabrication of Conducting Polymer Microtubules and Hollow Microspheres on Neural Microelectrode Arrays

1. Introduction

Micro/nanostructured conducting polymers have attracted attention because of their novel, unique properties and a series of biomedical applications, such as sensors and actuators. In our previous work, template synthesis method has been introduced and applied to chemical and electrochemical synthesize micro/nanotubules of conducting polymers using micro/nano-porous membranes as template. Nanomushrooms and nanohairs conducting polymers of polypyrrole (PPy) have been successfully electrochemical polymerized on the electrode site of neural probe [1, 2]. The main advantage of this method is that the length and diameter of the resulting nanostructured conducting polymers could be controlled by the selected porous membranes. Recent advances in materials science and molecular biology have shown us that nature used molecular self-assembly to construct microstructures of biomaterials. More and more research group has synthesized miro/nanofibrous materials using surfactant assemblies as a template [3, 4]. Compared to the template synthesis method, surfactant-mediated method is simple and cheap because no micro-or nano-porous membranes are used, furthermore, it is not necessary to remove the membrane after polymerization.

In this quarter of research, we describe the spectacular growth of microtubules PPy and hollow microspheres poly(3,4-ethylenedioxythiophene) (PEDOT) in the present of β-naphthalenesulfonic acid (β-NSA) as a dopant and self-assembling template, and studied their morphology and electrical properties. As different from previous sample preparation, the aqueous solution of pyrrole (Py) or 3,4-ethylenedioxythiophene (EDOT) mixed with β-NSA was stirred at room temperature for half hour and ultrosonificated for at least 20 minutes at 0 – 5 °C (ice bath). The resulting mixture look likes an emulsion which may be due to surfactant characteristics of the β-NSA dopant.

2. Results

2.1. Morphology

Fig.12 are optical micrographs showing that both PPy and PEDOT doped with β-NSA can be deposited onto the gold coated electrode sites. The black PPy/β-NSA was formed directly over the conducting sites, which were consistent with their oxidized, electrically conductive state. PEDOT films were brownish-black in appearance, it can bee seen that PEDOT coatings were deposited on the electrode sites and further spread out of the sites with increasing polymerization time.

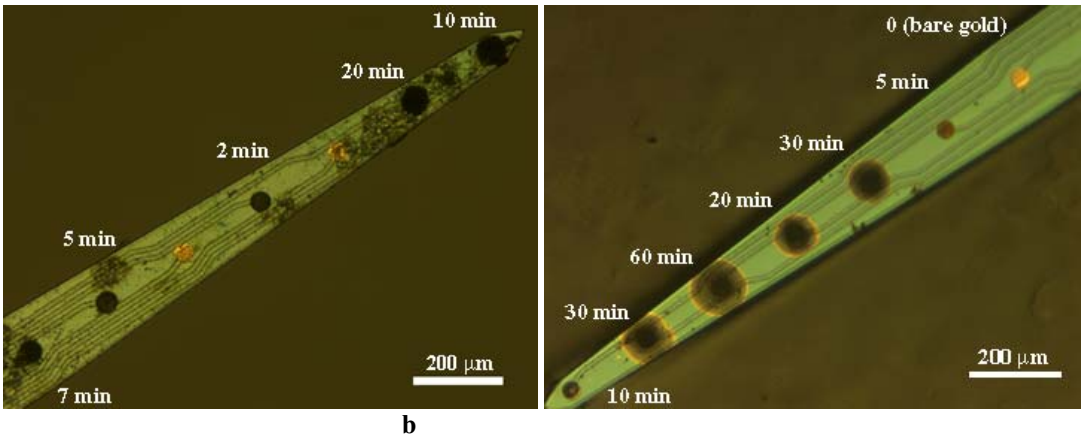

a **b**

Fig. 12 Optical micrographs of PPy and PEDOT coated on the electrode sites as a function of different polymerization time using β-NSA as a dopant. (a) PPy/β-NSA, Py: 0.53 mol L^{-1} and β-NSA: 0.57 mol L^{-1}; (b) PEDOT/β-NSA, EDOT=β-NSA: 0.02 mol L^{-1}; Current density: 0.5mA/cm^2.

To study the surface morphology of the PPy/β-NSA and PEDOT/β-NSA coated on the electrode, SEM was used. In general, only granular or fibrillar morphology was observed for conducting polymers synthesized by conventional chemical or electrochemical polymerization although the morphology depends on the polymerization method and conditions. The morphology of both PPy and PEDOT doped with poly (styrene sulfuric acid) (PSS) coated on the neural probe has been extensively studied in our previous work [5, 6], and the typical nodular structure has been observed. However, microtubules PPy and microspheres PEDOT were obtained in the presence of β-NSA as a dopant in this study (Fig. 13). For PPy, uniform PPy/β-NSA microtubules 0.2 ~ 1.5 μm in diameters and about 3.0 ~ 10 μm in length were obtained (Fig. 13a). The size of the microspheres of PEDOT doped with β-NSA is about 0.5 ~ 1.5 μm in diameter (Fig. 13b). Some broken microtubules and microspheres are observed in the SEM images (Fig. 14, red arrow), which indicates they are hollow. The results also showed that PPy/β-NSA microtubules could only be deposited on the neural probes by electrochemical polymerization at a high concentration of β-NSA surfactant (0.57 mol L^{-1}). This also can be seen from PEDOT doped with β-NSA that the hollow microspheres (green arrow) and bottlelike structures (red arrow) were both observed at high mole ratio of β-NSA (EDOT/β-NSA = ¼) (Fig. 14). As we mentioned in experimental part, the aqueous solution of Py and β-NSA, EDOT and β-NSA looks like an emulsion due to the surfactant characteristics of the β-NSA dopant. β-NSA has a characteristic amphiphilic structure with a hydrophilic $–SO_3H$, a dopant to PPy or PEDOT, and hydrophobic naphthalene ($-C_{10}H_7$). NSA is a typical surfactant and micelles can be formed in its aqueous solution. In fact, β-NSA acts as hydrotrope and anionic surfactant, which increases the solubility of organic compounds in water [7]. Therefore, Py and EDOT could be dissolved in β-NSA solution, and β-NSA tended to form micelles in high concentration. So, it is reasonable to assume that these micelles play an important factor in controlling the morphology of resulting microtubules of PPy/β-NSA and hollow microspheres of PEDOT/β-NSA. The β-NSA micelles not only could be considered as a template, but also act as a dopant. It is not necessary to remove after the polymerization.

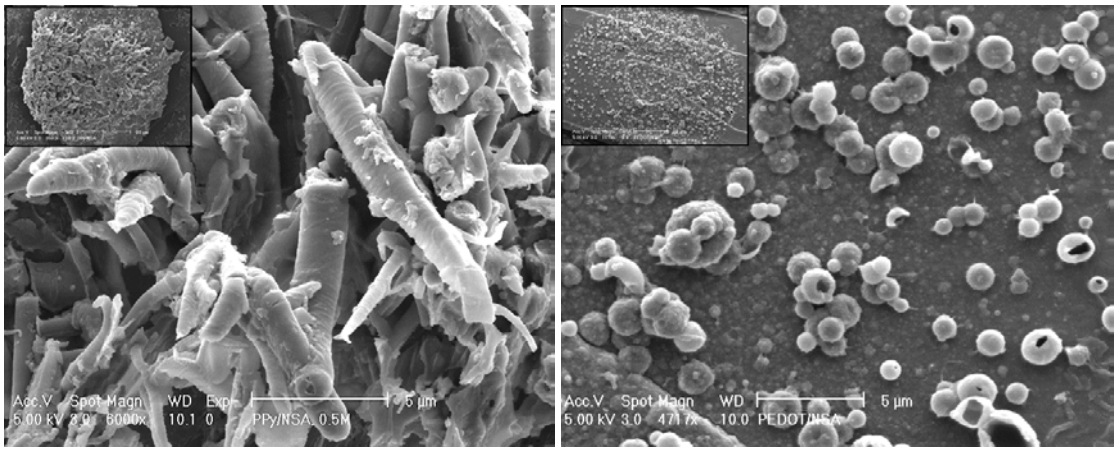

a **b**

Fig. 13 SEM images of PPy microtubules and PEDOT hollow microspheres electrochemical deposited on the neural probes. (a) PPy/β-NSA, Py: 0.53 mol L^{-1} and β-NSA: 0.57 mol L^{-1}; (b) PEDOT/β-NSA, EDOT=β-NSA: 0.02 mol L^{-1}; Current density: 0.5 mA/cm^2, polymerization time: 30 minutes.

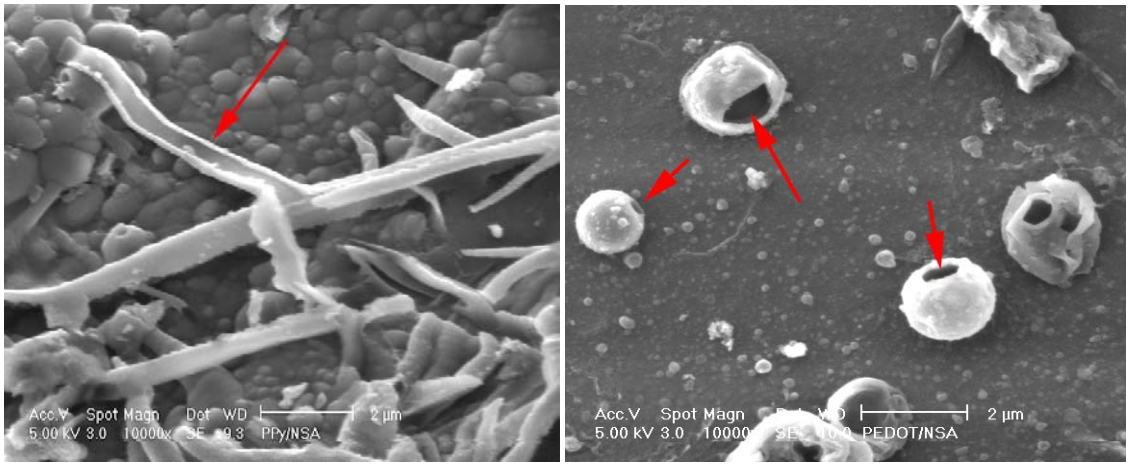

a **b**

Fig. 14 Typical SEM images of the "opened" PPy/β-NSA microtubules (a) and "hollow" PEDOT/β-NSA microspheres. Both deposition charge: 21.6 µC.

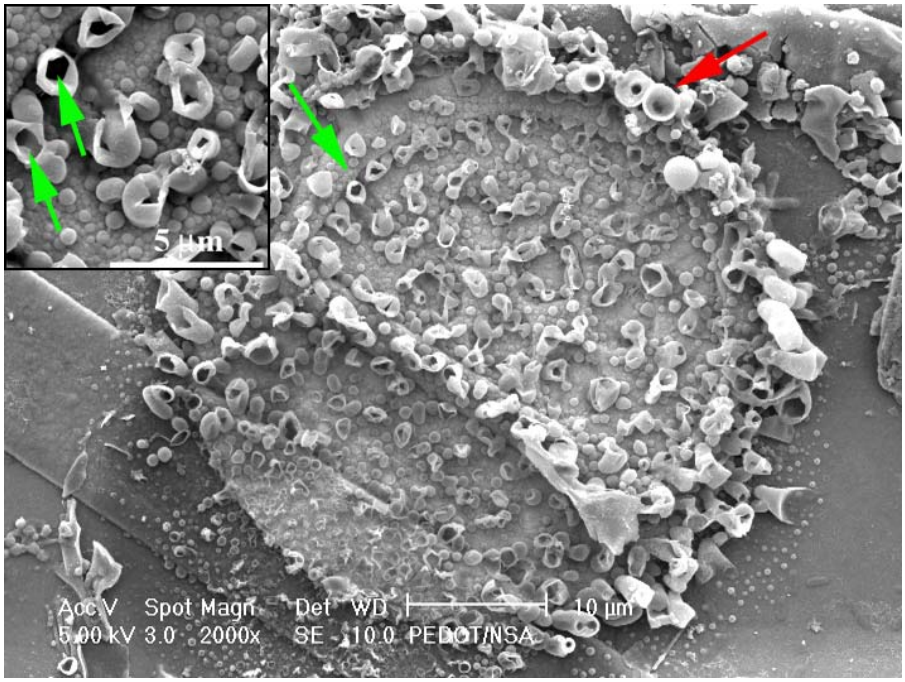

Fig. 15 SEM image of PEDOT/β-NSA microstructure electrochemical polymerized for 20 minutes on the electrode site at a current density of 0.5 mA/cm^2, the concentration of EDOT and β-NSA is 0.02 mol L^{-1} and 0.08 mol L^{-1}

2.1. Electrical Properties

The electrical properties of PPy and PEDOT coatings were measured using Electrochemical Impedance Spectroscopy (EIS) and Cyclic Voltammetry (CV). EIS involves measuring the electrode impedance (characterized by a magnitude (|Z|) and phase angle (θ)) over a spectrum of frequencies. Information about the system under test is obtained by comparing the input signal to the output signal. Magnitude and phase information are measured directly. Using these data, we can get qualitative and quantitative information about the electrical properties of the system over a large range of frequencies as well as the morphology of the electrode-medium interface. Fig. 16 shows the

impedance spectra of PPy/β-NSA and PEDOT/β-NSA coated electrode sites with an uncoated gold electrode spectrum as a control. It was found that the impedance of the PPy/β-NSA coated electrodes were significantly magnitude one order lower than that the uncoated gold electrodes within the whole frequency range (Fig. 16a). This can be explained by the high conductivity of the polymer coatings and more important by increasing the interfacial area. For the PEDOT doped with β-NSA, the impedance was much lower (two orders) than PPy doped with β-NSA in the whole range of frequency. As we know, for a capacitor, the impedance is purely imaginary, the current is out of phase with the voltage by 90°, and the phase angle is 90°. However, for a resistor, the impedance is real, the current and voltage are in phase and the phase angle is 0°. For a system composed of some combination of these two components, a large phase angle value indicates that the impedance is predominantly capacitive, while small angle values are resistive. The phase plot of the impedance spectroscopy (Fig. 5b) showed that the phase was around 80 º for bare gold, which means the electrode was close to a pure capacitor. However, after coating with PPy and PEDOT, the phase angle decreased to 20 ~ 30 º for PPy/β-NSA at low frequency range (<1 kHz), ~ 50 º at high frequency, and 10 ~ 5 º for PEDOT/β-NSA above1 kHz, which was an indication of a more resistive electrode.

A Nyquist plot shows the imaginary part of the impedance (ImZ) vs. the real part (ReZ). As can be seen from Fig. 16c, the steep straight line of bare gold is typical of a pure capacitor. However, after coating with conducting polymer, the plot of PPy/β-NSA was straight near 45°over the whole range of frequency. This is close to the typical Warburg impedance with constant phase of 45°, which shows the frequency dependence of the impedance on mass transfer of ions to the interface, while the trajectory of PEDOT/β-NSA was not straight, and is higher than 45° over the whole range of frequency. This can probably be explained by the rough, highly textured surface of PEDOT/β-NSA which adds complexity and non-uniformity to the frequency dependent impedance [8].

To optimize the electrical properties of PPy and PEDOT coated electrode, the impedance magnitudes at 1 kHz were measured as a function of deposition charge (Fig. 6). Results show that both impedance magnitude of PPy/β-NSA and PEDOT/β-NSA deposited on gold electrodes varied non-linearly as the amount of the material on the electrode changed. The impedance initially decreased sharply as increasing the deposition charge, then the rate of decrease slow down and reached a minimum at about 10 μC, and then the impedance gradually increased a lit bit more as increasing the polymerization time (deposition charge). However, the impedance of PEDOT/β-NSA decreased sharply than that of PPy/β-NSA, and reached a much lower impedance magnitude at the same deposition charge. All correspond to the most fuzzy, highly surface area of PEDOT coatings on the electrode site, since it provides the highest interfacial area for charge transport.

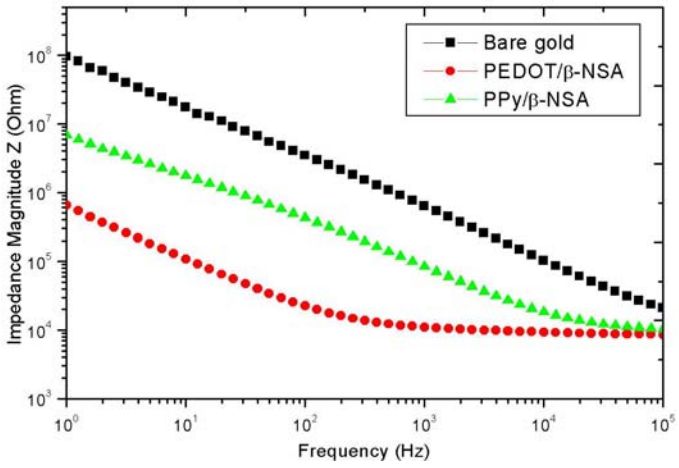

a

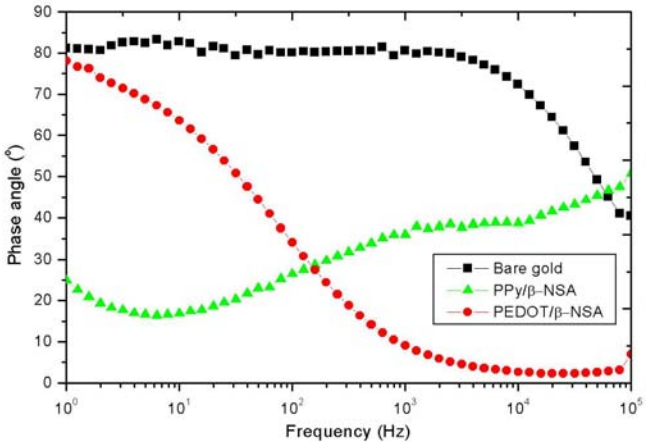

b

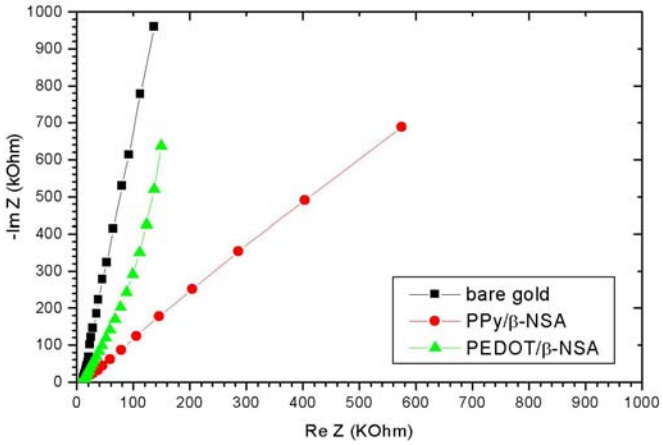

c

Fig. 16 Impedance spectroscopy of bare gold, PPy/β-NSA coated and PEDOT/β-NSA coated electrodes, The uncoated gold electrode area is 1250 μm^2. (a) Magnitude of impedance as a function of frequency, (b) Phase angle of impedance as a function of frequency, and (c) Nyquist plot.

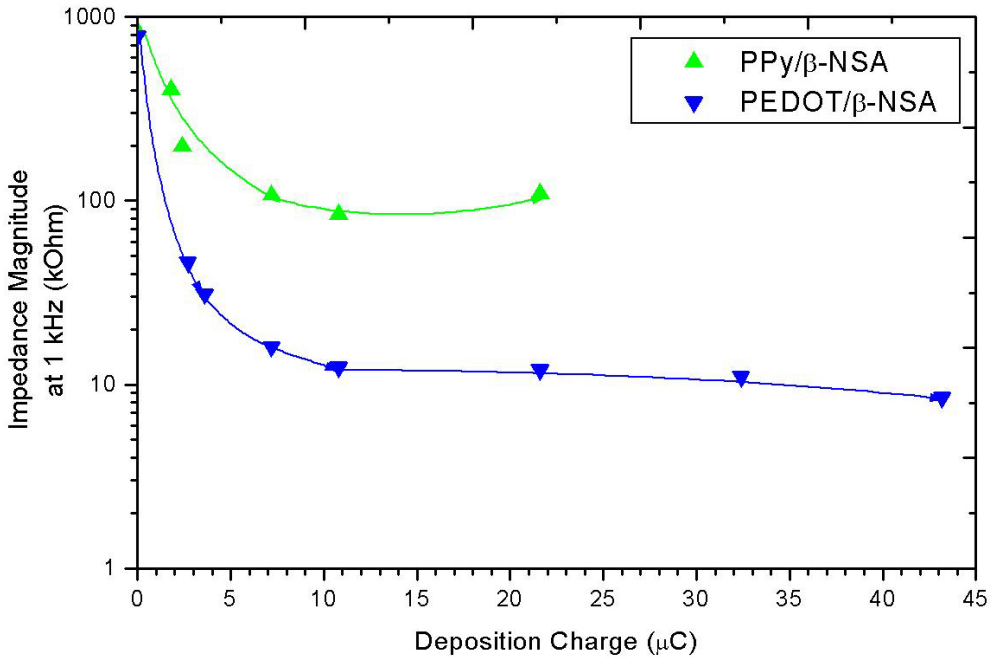

Fig. 17 Impedance magnitude of PPy/β-NSA and PEDOT/β-NSA coated on the electrode at 1 kHz as a function if deposition charges, the gold electrode site is 1250 μm^2.

The electrochemical stability of PPy/β-NSA and PEDOT/β-NSA coatings was tested using CV. The coating deposited on the microelectrode was swept through a potential of -0.9 to 0.5V vs. SCE with scan rate of 0.1 V/s for up to 120 cycles. During each cycle, the film undergoes reduction and oxidation with corresponding movement of ions in or out of the coating. The peak potential indicates when the reaction takes place; the peak current indicates the number of mobile charge carriers in the coating, and the enclosed area of the curve is proportional to the charge capacity. In the case of PPy/β-NSA (Fig.18a), the enclosed area (proportional to charge capacity) decreased much more as compared with the original after 40 cycles, which is related to the instability of the polypyrrole because its significant amount of α-β' coupling in polypyrrole provides defect sites along the polymer chain. PEDOT/β-NSA on the other hand, showed a significant improvement in the electrochemical stability of the coating. As shown in Fig. 18b, the area encompassed by the CV curve didn't shrink for 40 cycles and then conserved the shape until the 120th cycle. This is a good indication of the electrochemical stability of the PEDOT. This stronger stability has been shown elsewhere in our previous report doped with PSS.

In addition, we found that the oxidation potential for PEDOT/β-NSA is around -0.6 V vs. SCE, which is much lower than that of PPy/β-NSA (-0.4 V. vs. SCE), PPy/PSS (0.1 V. vs. SCE) [5] and PEDOT/PSS (-0.4 V. vs. SCE) [6]. This lower reduction potential means a higher resistance to any biological reducing agents in the living tissue. This property is highly desirable in chronic implantation of neural probes.

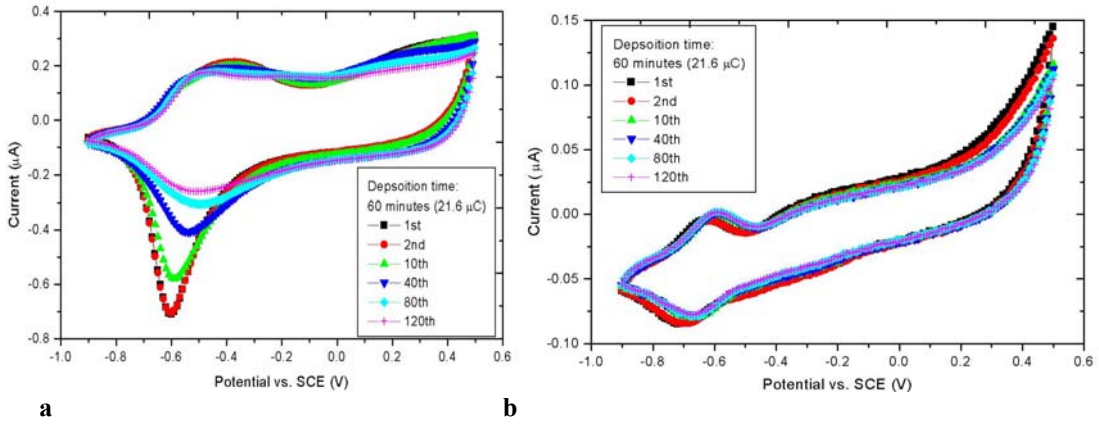

Fig.18: CV of (a) PPy/β-NSA and (b) PEDOT/β-NSA coated on the electrode site. The uncoated gold electrode area is 1250 μm^2, scan rate 0.1 V/s.

Conclusions:

Microtubules of PPy/β-NSA and hollow microspheres of PEDOT/β-NSA were electrochemically deposited on the neural probes using surfactant assemblies as a template. Influence of the polymerization conditions on the morphologies of PPy/β-NSA and PEDOT/β-NSA was investigated. Electrical properties have been studied by electrochemical impedance spectroscopy and cyclic voltammetry. The results show that PEDOT/β-NSA has two orders of magnitude lower impedance over the whole range of frequency, while PPy/β-NSA only decreased the impedance by one order of magnitude. The impedance data were consistent with a fuzzy, high surface area morphology that is demonstrated in SEM images. Also, the CV results indicate that PEDOT/β-NSA is more electrochemically stable than PPy/β-NSA.

References

1. J. Yang and D. C. Martin, "Electrochemical Polymerization of Conducting Polymer Coatings on Neural Prosthetic Devices: Nanomushrooms of Polypyrrole Using Block Copolymer Thin Films as Templates", *MRS Proceeding*, Vol.734 (2003)

2. J. Yang, D. C. Martin, "Electrochemical Deposition of Nanostructured Conducting Polymer Coatings on Neural Prosthetic Devices", *Bull. of Am. Phys. Soc*., Vol. 48, 942, 2003

3. Y.S. Yang and M.X.Wan, "Microtubules of Polypryrrole Synthesized by an Electrochemical Templated-free Method". *J. Mater. Chem*., 11, 2022 (2001)

4. M. Harada and M. Adachi, "Surfactant-mediated Fabrication of Silica Nanotubes", *Adv. Mater.,* 12, 839 (2000)

5. X. Y. Cui, V. Lee, Y. Raphael, J. Wiler, J. Hetke, D. J. Anderson and D. C. Martin, "Surface Modification of Neural RecordingElectrodes with Conducting Polymer/Biomolecule Blends", *J. Biomed. Mat. Res*, 56, 261, 2001.

6. X. Y. Cui and D. C. Martin, "Electrochemical Deposition and Characterization of Poly(3,4-ethylenedioxythiophene) on Neural Microelectrode Arrays", *Sensors and Actuators B*, 1-11, 6581 (2002)

7. G. Hons, *in Anionic Surfactant Organic Chemistry*, Vol. 56, eds. Helmut W. Stache, Marcel Deller, Inc., New York, 1995, P.82.

8. T.Komura, S.Goisihara, T. Yamaguti, K. Takahasi, *J. Electroanal. Chem*., 456, 121 (1998)

Impedance of Electrochemically Deposited Polymer Films as a Function of Deposition Charge (Thickness)

We have now generated information about the electrical impedance of a variety of electrochemically deposited polymer films prepared in our laboratory. Figure 19 shows a compilation of these results, as we have reported earlier in this report and in our previous progress reports. In all cases, there is a dramatic initial drop in the impedance as the film grows thicker, followed by an eventual increase in the impedance when then film is sufficiently thick. The typical early decrease in impedance is two orders of magnitude, for an optimal applied charge that typically ranges from 5-30 μC. We have qualitatively interpreted these results as due to the increase in effective surface area of the film in the initial stages of growth, followed by a subsequent increase in impedance as the film thickens. We are actively working to develop models to explain this behavior more quantitatively, based on our morphological observations of the films by SEM and optical microscopy. It should also be appreciated that there seems to be a systematic difference between the value of current required in the new AutoLab system to get the same thickness of film as needed with the old Gamry instrument in the EECS laboratory. We currently estimate that the total charge required to get the same amount of polymer deposition in the AutoLab is about 17 times greater than in the Gamry. Since the differences appear to be systematic, we are looking for a means to calibrate the devices. In the meantime the charge is likely best considered as an "apparent" value.

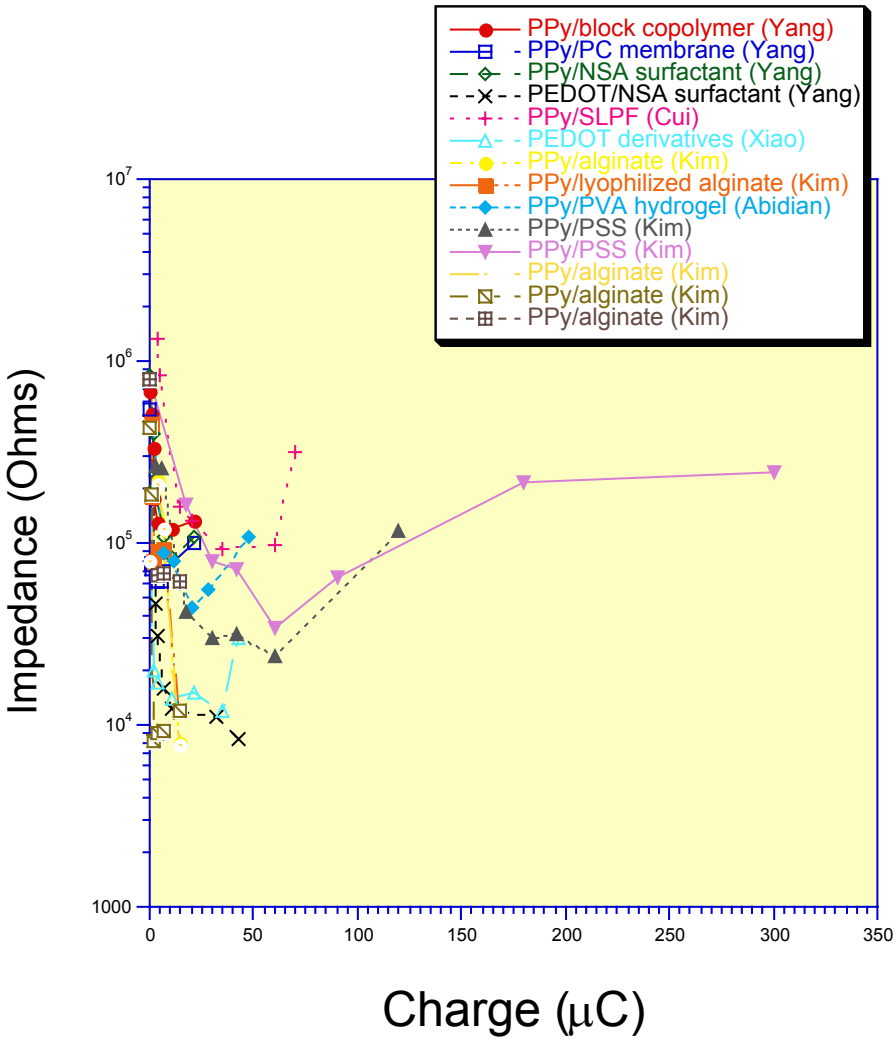

Figure 19: Compilation of the impedance at 1 kHz as a function of charge for a variety of electrochemically deposited polymer films prepared in our laboratory.

Quarterly Progress Report for the period February 1, 2003 – April 30, 2003
Report #6, April 30, 2003

Keck Center for Tissue Engineering
Patrick A. Tresco, P.I.
University of Utah subcontract for N01-NS-1-2338

OVERVIEW

In this progress report, we discuss the results of a quantitative study of the brain tissue reaction hydrogel coated electrodes compared to control, that was described qualitatively in the last report (Report #5, January 31, 2003). Specifically, we conducted an unbiased analysis (described below) of the spatial distribution of GFAP and neurofilament immunoreactivity adjacent to the tissue cavities that remained after retrieval of two types of hydrogel-coated electrodes and uncoated controls. The results study call into question two points that we made in the last report, namely that,: i) hydrogel-coated electrodes can reduce the extent of gliosis surrounding an implanted electrode, and, ii) there is no reduction of neurofilament staining adjacent to hydrogel-coated electrodes.

Our most recent study suggests that there is likely no difference in GFAP immunoreactivity between the various hydrogel coated electrodes compared to control, and that regardless of coating, there is a significant reduction in neurofilament immunoreactivity for distances up to 200 microns around implanted tethered electrodes. The details are provided in the following sections.

MATERIALS AND METHODS

Please refer to the 5th quarterly report (January 31, 2003) progress report for all methods related to the hydrogel coatings and implantation methodology. Line profile analysis was conducted as described in the 4th quarterly report (October 31, 2002), and for clarity is replicated below. All digital images used for sample data were collected by confocal microscopy using identical settings, and only one optical section was used to generate a single image. Once average line profiles were generated for each condition, a background correction was applied. The correction corresponded to normal tissue immunoreactivity from the same brain section. All data points at the tail end of each line profile, between 500 and 700 microns away from the implant interface, were averaged and this average value was subtracted from each data point between 0 and 500 microns. In this manner, normal immunoreactivity corresponds to an intensity value of approximately 0. The validity of this correction method was confirmed by comparing averaged intensity values with line profiles generated from the same brain slices in the contralateral hemisphere. No difference was observed for both GFAP and neurofilament staining.

Unbiased quantitative analysis of tissue response to implanted materials. We have developed a method for collecting a series of line-based intensity profiles from captured digital images. The fluorescence intensity of any stained section can be quantified and expressed as mean pixel intensity as function of distance from the implant interface.

Using this approach it is possible to compare the response as a function of any given variable using standard and objective criteria that can be compared with statistical methods. Serial brain sections are first collected. For any desired immunostain, a series of evenly spaced sections along the implant interface are batch stained using the same solutions and conditions, and then mounted. Images of immunostained sections are viewed and captured by a PMT device mounted on a laser scanning confocal microscope. Images are stored as unsaturated 8 bit TIF files. For any given session where many images are captured, the same acquisition settings are used (PMT voltage, scan time, capture resolution, laser intensity, etc.). The settings are determined so that all images are of sufficient brightness for viewing, but the vast majority of pixels are not saturated. Single optical sections are collected and stored for each sample.

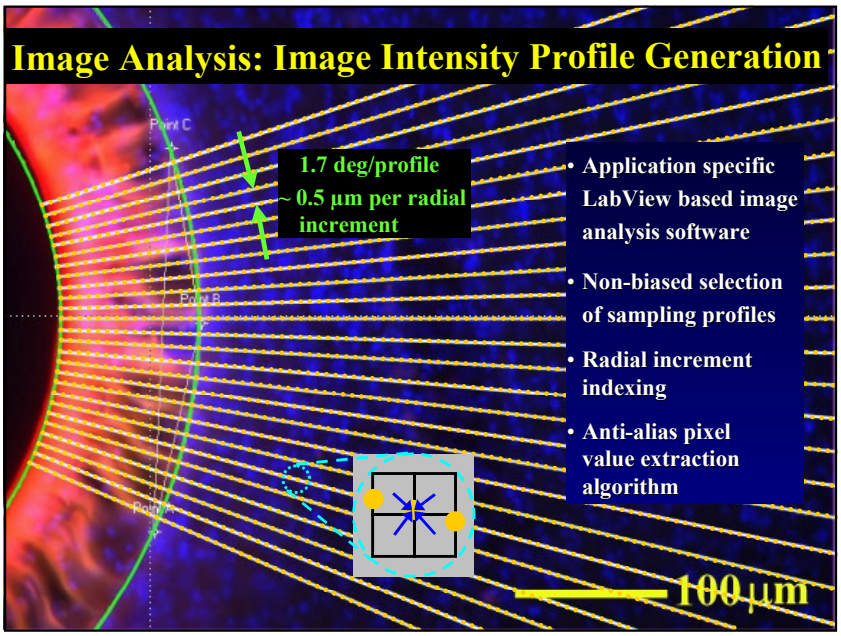

Figure U6-1. Sample radial line array of a digital image. A horizontal section of a hollow fiber membrane whose lumen was loaded with a Texas-Red labeled lysine fixable dextran.

The measurement approach uses three points to delineate a reference arc at the interface of an implant. The angular location and size of the reference arc is adjustable enabling exclusion of defects that may be present in the image such as air bubbles. Once a reference arc is delineated intensity sampling profiles are generated at a density of ~1.7 deg per profile and are typically set to acquire between 20-35 profiles per image captured (Figure U6-1). Profiles extend normal to the delineated arc and are radially indexed in 0.5µm increments. At each radial increment an anti-alias pixel extraction algorithm is applied to derive an intensity value based on a weighted averaging of pixels in nearest proximity. A single image intensity profile is then calculated by averaging all coinciding increments of the sampling profiles generated and is performed simultaneously for all color channels (RGB) present in the selected image. The average image intensity profile along with its radial indices is then saved in a text format file for later numerical analyses. Following profile analysis of all experimental group images, an average probe intensity profile can be calculated for each of the sample group and antibody utilized.

It is important to note that this does not represent the true implant tissue interface in those cases were adherent tissue is removed with the retrieved electrode and is important to consider to obtain the entire picture of reactivity.

RESULTS

Astroctye Response to Hydrogel-Coated Arrays . Qualitative assessment of the astrocyte response was conducted using antisera to GFAP. We observed that the degree of astrocyte reactivity in tissue sections appeared lower around the cavity that remained following retrieval of hydrogel coated arrays compared to that observed adjacent to the smaller cavity created by retrieved uncoated controls. In some samples, the characteristic hypertrophied interwoven astrocyte barrier was absent. In order to further examine this reaction, an unbiased quantitative line profile analysis was conducted on a series of digital confocal micrographs. Both hydrogel coatings demonstrated a reduction in GFAP immunoreactivity compared with uncoated controls. The reduction in GFAP was evident both in the peak GFAP response within 50 microns of the electrode interface and throughout the adjacent tissue to a distance of approximately 450 microns away (Figure U6-2). The lyophilized hydrogel coating had the most notable difference, with an approximate 50% reduction in peak GFAP intensity.

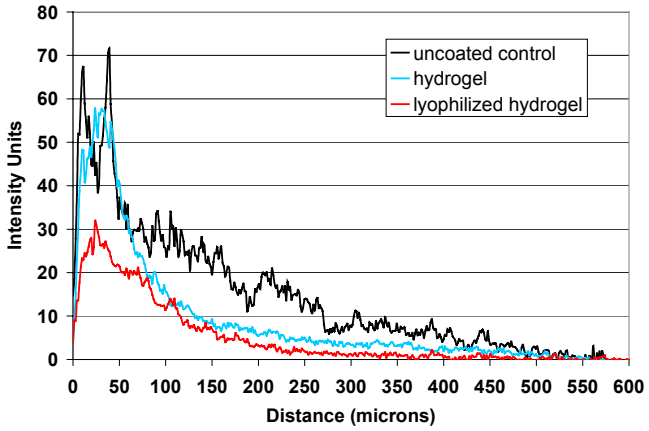

Figure U6-2. Average GFAP intensity as a function of distance from electrode interface.

It is important to note that these measurements provide an average, and as a result, specific relevant phenomena may be overlooked. While uncoated control electrodes demonstrated a consistent degree of astrocyte reactivity, there was a greater variability among animals implanted with coated arrays. The typical gliotic reaction around the implant interface of some hydrogel or lyophilized hydrogel-coated arrays was notably absent. The mechanism for this remains unclear, and before further interpretation can be forwarded, it is important to examine the possibility that the observation may be experimental artifact. This may occur when the implant is retrieved and the interface is not properly preserved. With respect to the GFAP response, we believe that this is a valid concern. In some but not all retrieved electrodes, we observed adherent GFAP+ cells along the electrode shaft. Indeed, the lyophilized coatings, which had the lowest measured gliotic response in the adjacent tissue, also contained GFAP+ material on the retrieved electrodes. In contrast, no GFAP immunoreactive material was found on uncoated electrodes, only numerous microglia and macrophages. Thus, the graph of reaction to the lyophilized arrays in Figure U6-2 may represent a normal gliotic response like that seen for uncoated arrays, but we simply observe the tail end of the response,

which has been shifted to the left due part of the interface being removed as a result of implant retrieval. Attempts will be made to modify the histological approach to preserve the interface and eliminate this complication.

Neuronal density adjacent to hydrogel-coated arrays. A similar line profile analysis was performed on tissue sections immunostained for neurofilament. Unlike the GFAP reaction, little difference in the pattern and abundance of neurofilament was observed between coatings and control. Here we observed a reduction in neurofilament that extended up to 200 microns away from the implant interface (Figure U6-3), again we need to be cautious at how we use this comparison for the same reasons, that is the data for the hydrogel –coated electrodes actually begins at a greater distance from the recording sites. 0 distance in Figure U6-3 actually represent the edge of the cavity that remains after the implant has been retrieved. Implants that are well integrated may extract more tissue from the implant site during the retrieval process.

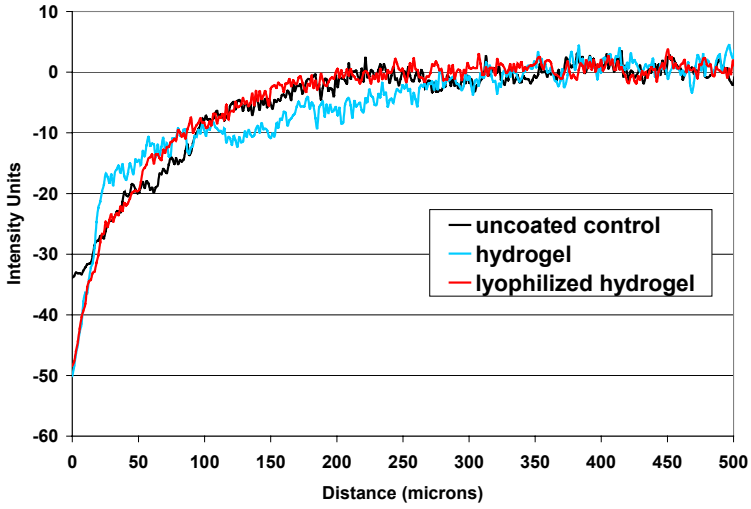

Figure U6-3. Reduction in neurofilament adjacent to implanted uncoated and hydrogel-coated electrodes.

The degree of neurofilament reduction has potentially important implications for electrode function, as the limit of useful range of recording capability of this type of electrode is estimated at approximately 150 microns. If normal neuronal density is required to achieve stable recording, our data indicates that such conditions exist at distances beyond 200 microns from the recording sites. This is likely to be a conservative estimate for the hydrogel-coated arrays, as the implant cavity was significantly larger and by our crude estimates may displace the electrode by as much as an additional 180 microns away. It is also important to note that we found little evidence of neurofilament positive material on any type of retrieved electrode to date. We have previously reported a modest reduction of neurofilament staining within approximately 15 microns of untethered and uncoated electrode arrays, which was in agreement with previous studies of others. We speculate that the striking difference observed here is likely due to tethering of the implant.